

## Extending the ICRF to Higher Radio Frequencies – Imaging and Source Structure

David A. Boboltz <sup>1</sup>, Alan L. Fey <sup>1</sup>, Patrick Charlot <sup>2</sup>, Edward B. Fomalont <sup>3</sup>,  
Gabor E. Lanyi <sup>4</sup>, Liwei D. Zhang <sup>4</sup>, KQ VLBI Survey Collaboration <sup>5</sup>

<sup>1)</sup> *U.S. Naval Observatory*

<sup>2)</sup> *Bordeaux Observatory*

<sup>3)</sup> *National Radio Astronomy Observatory*

<sup>4)</sup> *Jet Propulsion Laboratory, California Institute of Technology*

<sup>5)</sup> *Multiple Institutions*

*Contact author: David A. Boboltz, e-mail: [dboboltz@usno.navy.mil](mailto:dboboltz@usno.navy.mil)*

### Abstract

We present imaging results and source structure analysis of extragalactic radio sources observed using the Very Long Baseline Array (VLBA) at 24 GHz and 43 GHz as part of an ongoing NASA, USNO, NRAO and Bordeaux Observatory collaboration to extend the International Celestial Reference Frame (ICRF) to higher radio frequencies. The K/Q-band image database now includes images of 108 sources at 43 GHz (Q-band) and images of 230 sources at 24 GHz (K-band). Preliminary analysis of the observations taken to date shows that the sources are generally more compact as one goes from the ICRF frequency of 8.4 GHz to 24 GHz. This result is consistent with the standard theory of compact extragalactic radio sources and suggests that reference frames defined at these higher radio frequencies will be less susceptible to the effects of intrinsic source structure than those defined at lower frequencies.

### 1. Introduction

The K/Q-band VLBI Survey is part of an ongoing NASA, USNO, NRAO and Bordeaux Observatory collaboration to extend the International Celestial Reference Frame (ICRF) to higher radio frequencies [1]. The long term goals of this program are a) to develop higher frequency reference frames for improved deep space navigation, b) to extend the VLBA calibrator catalog at 24 and 43 GHz, c) to provide the benefit of the ICRF catalog to new applications at these higher frequencies and d) to study source structure variation at 24 and 43 GHz in order to improve astrometric accuracy. Here we describe the production of the K/Q-band image database and provide some preliminary results on extragalactic source structure at higher frequencies from the analysis of the image data.

### 2. Observations

Observations for the K/Q-band VLBI Survey were made using the 10 stations of the VLBA at K-band (24 GHz) and Q-band (43-GHz) under experiment names BR079 and BL115. Table 1 summarizes program observations recorded to date. All observations were taken using short duration “snapshots” over a number of different hour angles in order to maximize the  $u$ - $v$  plane coverage. Data were recorded using eight 8-MHz bands. The data were correlated at the NRAO correlator in Socorro, NM. For the first two experiments BR079A and BR079B the same 65 ICRF sources

were observed in order to test the repeatability of the observations. Experiment BR079C observed 67 ICRF sources with 24 of those overlapping sources from previous experiments. Experiment BL115A was a K-band only experiment designed to search for additional high-frequency sources. Experiment BL115B was again a K/Q-band experiment in which 70 sources were observed with roughly 1/3 of the sources overlapping with previous experiments.

Table 1. Summary of K/Q-band VLBI observations.

Experiment Code	Observation Date	Observing Band(s)	No. of Sources Observed	No. of Sources Imaged	Notes
BR079A	15-May-02	K and Q	65	65	65 ICRF sources
BR079B	25-Aug-02	K and Q	65	65	Same 65 sources as BR079B
BR079C	26-Dec-02	K and Q	67	67	24 sources overlapping BR079A,B
BL115A	22-May-03	K only	249	184	122 new sources
BL115B	13-Sep-03	K and Q	70	N/A	Partially imaged

### 3. Data Reduction and Imaging

Data from the K/Q-band VLBI program were calibrated using the Astronomical Image Processing System (AIPS) which is maintained by the National Radio Astronomy Observatory (NRAO). An initial amplitude calibration was performed using the system temperature measurements recorded during the observations and the VLBA antenna gains supplied by NRAO. To correct the residual delays and rates, a fringe-fit was performed within AIPS. Post fringe-fit data reduction was accomplished using the Caltech DIFMAP software package. The data were self-calibrated and imaged using the hybrid mapping technique to correct for any residual amplitude and phase errors in an automated iterative process. Images and visibility data for sources at K- and Q-band may be obtained at the USNO Radio Reference Frame Image Database <http://www.usno.navy.mil/RRFID>.

## 4. Results

### 4.1. Source Compactness

One of the primary goals of the imaging part of the K/Q-band VLBI program is the determination of source structure and its effect on astrometry at higher frequencies. A useful indicator of the degree to which a source may be considered compact is the ratio of the source core flux density to the total flux density in the image or the source compactness. By this indicator, a point-like source, one in which all of the flux was contained in the core, would have a ratio of 1.0. Source compactness (core/total flux density) can be determined using either the CLEAN components from the images themselves or Gaussian model fits to the features in the image. In the case of Gaussian models, the core is defined as the model component fit to the image feature with the smallest angular size, and the total flux density is defined as the sum of the flux densities from all Gaussian components. For the CLEAN components case, the core is defined as the sum of the CLEAN components within one synthesized beam, and the total flux density is defined as the sum of all positive CLEAN component flux densities in the image.

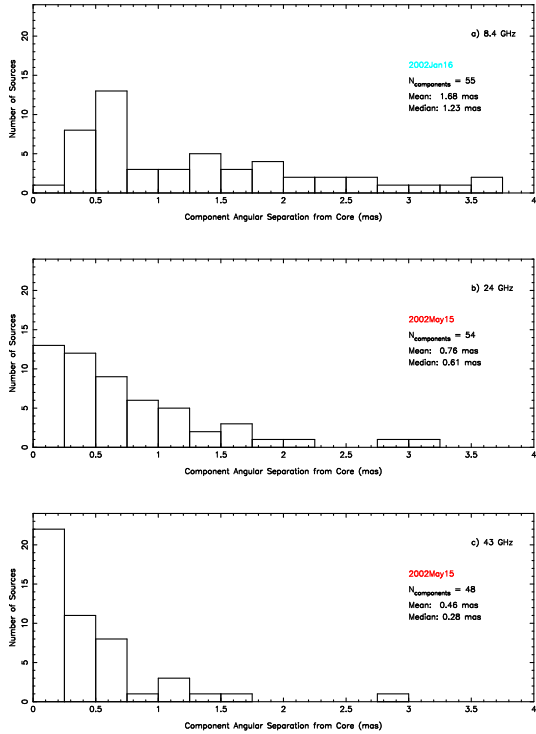


Figure 1. Distribution of Gaussian component angular separation from the core for the 28 sources common to K/Q-band experiment BR079A and VLBA X-band data observed January 16, 2002.

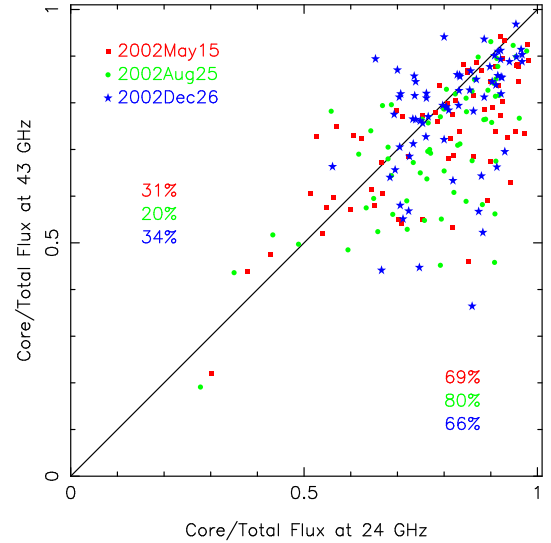


Figure 2. Comparison of the core/total flux as derived from the CLEAN components for the 108 sources observed at 24 GHz and 43 GHz in experiments BR079A, B and C

Figures 1–4 demonstrate the various ways in which the Gaussian/CLEAN components and the source compactness can be utilized. Figure 1 shows a histogram of angular separations of the Gaussian components from the core component for the K/Q-band experiment BR079A. This figure demonstrates the trend toward smaller source angular extents with increasing observing frequency. However, a comparison of the source compactness at 24 and 43 GHz (Figure 2), indicates that even though the total angular extent of the source is smaller at higher frequencies, the sources are really no more compact at Q-band than at K-band. Figure 2 plots data from three experiments, BR079A-C. In this figure sources more compact at K-band lie below the diagonal line while sources more compact at Q-band lie above the line. The results are consistent for all three K/Q-band experiments analyzed thus far.

Shown in Figures 3 and 4 are the results from our K-band only survey (BL115A). Figure 3 plots a histogram of the source compactness. Figure 4 plots this source compactness as a function of source flux density. Preliminary results indicate that weaker sources appear to be more compact than their higher flux counterparts. This trend, however, could be a selection effect in the data and further investigation is required.

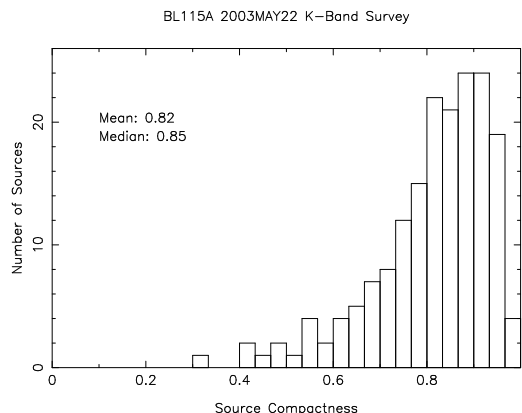


Figure 3. Histogram showing the source compactness (core/total flux) for the 184 sources observed at 24 GHz in experiment BL115A.

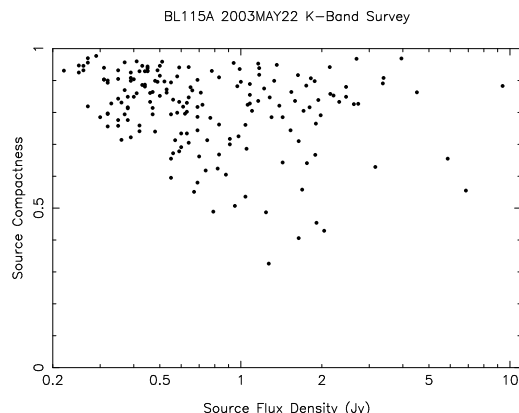


Figure 4. Source compactness (core/total flux) vs. source total flux density for the 184 sources observed at 24 GHz in experiment BL115A.

## 4.2. Structure Index

A second indicator of source quality is the “structure index” developed by Fey and Charlot [2, 3]. The structure index is defined as the median value of the corrections to the VLBI delay observables due to the source structure as measured in the image. Sources can be categorized by structure index with 1 and 2 indicating compact structure desirable for astrometry/geodesy, 3 being marginal, and 4 being unacceptable for use in astrometric/geodetic VLBI. Figures 5 and 6 compare structure index results from our K/Q-band observations with previously recorded X-band ICRF observations. In Figure 5, histograms showing the structure index at a) X-band, b) K-band, and c) Q-band are plotted. The K- and Q-band results are for the 65 ICRF sources from experiment BR079A, while the X-band results are from a nearby (in time) VLBA experiment with 28 ICRF sources overlapping BR079A. The results show a significant increase in the number of good (structure index of 1 or 2) sources from X-band,  $\sim 86\%$ , to K-band,  $\sim 97\%$ . There was no improvement in structure index from K-band to Q-band for this experiment. Figure 6 compares histograms of the source structure indices at X-band and K-band for 156 ICRF sources observed in experiments BR079A-C and BL115A. The X-band structure indices were derived from previous VLBA experiments. At X-band approximately 83% of the sources have structure indices of 1 or 2, while at K-band this number increases to  $\sim 95\%$ . This improvement in source structure at higher frequencies should translate to increased astrometric accuracy for the source positions and ultimately for a reference frame based on high-frequency radio observations.

## References

- [1] Jacobs, C. S., et al. 2003, The International Celestial Reference System: Maintenance and Future Realization, 25th meeting of the IAU, Joint Discussion 16, 22 July 2003, Sydney, Australia, 16,
- [2] Fey, A. L. & Charlot, P. 1997, ApJS, 111, 95.
- [3] Fey, A. L. & Charlot, P. 2000, ApJS, 128, 17

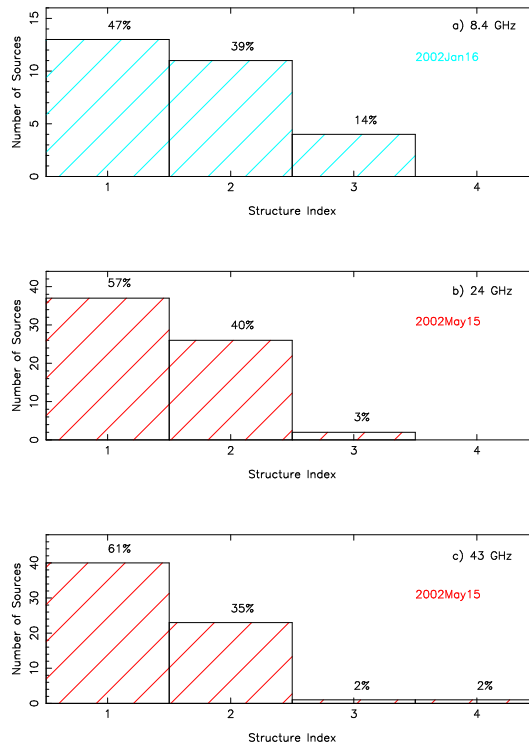


Figure 5. Distribution of structure indices for 28 ICRF sources at a) 8.4 GHz, and for 65 ICRF sources at b) 24 GHz, and c) 43 GHz. The 65 sources at 24 and 43 GHz are from BR079A observed 15 May, 2002. The 28 overlapping sources at 8.4 GHz are from a VLBA experiment conducted on 16 January 2002. Note the shift toward lower values as the observational frequency increases.

Distribution of Structure Index for 156 ICRF Sources

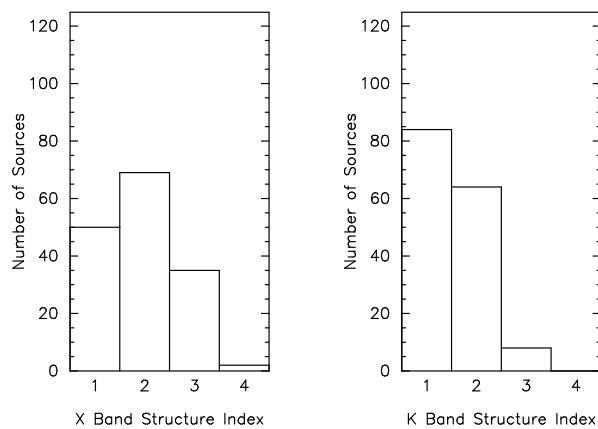


Figure 6. Distribution of structure indices for ICRF sources at 8.4 GHz (left panel) and 24 GHz (right panel). K-band structure indices are from experiments BR079A-C and BL115A. Note the shift toward lower structure indices from X-band to K-band.